APPLICATION OF MULTI-SYNCHROSQUEEZED GENARALIZED S-TRANSFORM IN SEISMIC TIME-FREQUENCY ANALYSIS

QIAN WANG[1], XUEHUA YANG[1], BO TANG[1], NAIHAO LIU[2,3] and JINGHUAI GAO[2,3]

[1] School of Mathematics and Statistics, Hubei University of Arts and Science, 296 Longzhong Road, Xiang Yang 410000, P.R. China.
wqlq668930@126.com, yangxuehua_0411@163.com.
[2] School of Electronic and Information Engineering, Xi'an Jiaotong University, 28 Xianning West Road, Xi'an 710049, P.R. China. Naihao_liu@mail.xjtu.edu.cn.
[3] National Engineering Laboratory for Offshore Oil Exploration, Xi'an Jiaotong University, 28 Xianning West Road, Xi'an 710049, P.R. China. jgao@mail.xjtu.edu.cn.

(Received October 8, 2022; revised version accepted December 23, 2022)

ABSTRACT

Wang, Q., Yang, X.H., Tang, B., Liu, N.H. and Gao, J.H., 2023. Application of multi-synchrosqueezed genaralized S-transform in seismic time-frequency analysis. *Journal of Seismic Exploration*, 32: 39-49

Time-frequency (TF) analysis is an important tool in seismic data processing that describes the frequency response of subsurface rocks and reservoirs. In this paper, we propose a new TF method to characterize the time-varying feature of seismic signals, the proposed method is based on a generalized S-transform and employs a multi-synchrosqueezing algorithm. The technique provides a highly energy-concentrated TF representation using a novel local estimation of instantaneous frequency. Synthetic and field data examples show that the proposed method has a superior performance in depicting strong time-varying signals and can be used to identify subtle stratigraphy with high resolution.

KEY WORDS: time-frequency analysis, multi-synchrosqueezing, generalized S-transform, reservoir characterization.

0963-0651/23/$5.00

INTRODUCTION

Seismic data are nonstationary in nature and has varying frequency content as a function of time. TF spectral analysis (also called spectral decomposition) plays a significant role in seismic data processing by transforming seismic traces to spectral amplitudes as a function of time and frequency. In this way, TF spectral analysis helps characterize frequency-dependent responses of subsurface rocks and reservoirs (Sinha et al., 2005). For instance, seismic low-frequency amplitude shadows can be used as a hydrocarbon indicator when high-frequency components are absorbed by a reservoir (Ebrom, 2004). In addition, TF spectral analysis can also be use for noise suppression, attenuation measurement and pore-pressure prediction (Reine et al., 2009). There are various TF methods for nonstationary signal analysis. Short-time Fourier transform (STFT) is one of the most commonly used approach and produces a TF spectrogram by applying the Fourier transform (FT) over a chosen time window. TF resolution of STFT is limited by the preselected window length. To overcome the limitations of STFT, the continuous wavelet transform (CWT) has been developed and is widely used in various engineering technology fields (Chakraborty and Okaya, 1995). However, the time-scale representation produced by CWT is not intuitive in seismic interpretation because the scale variable represents a frequency band. In recent years, the S transform (ST) (Stockwell et al., 1996) has become popular in seismic TF analysis due to its convenient computation via Fourier transform. The ST method can be considered as a hybrid of STFT and CWT. By employing a frequency-dependent Gaussian window, the ST provides a TF spectrum with multiresolution while maintaining a direct relationship with the Fourier spectrum. The ST also has the capacity of preserving phase information. Because of the uncertainty principle, the TF spectrum generated by these linear methods is often blurry, which makes it difficult to describe the time-varying features of a seismic signal accurately.

For quadratic methods, the Wigner-Ville distribution (WVD) (Jeffrey and William, 1999) is not affected by the uncertainty principle and can reduce energy diffusion dramatically. However, the cross-term involved in this procedure has no physical meaning restricts its application. To overcome these difficulties, a post-processing technique known as the reassignment (RM) algorithm (Auger and Flandrin, 1995) was proposed to improve the readability of TF representation (TFR). RM transfers the TF coefficients from their original position, to the center of gravity of energy distribution, to reduce energy confusion. However, the RM does not have the ability for signal reconstruction. The synchrosqueezing transform (SST) (Daubechies et al., 2011), originally introduced in audio signal analysis, is a promising tool for TF analysis. It captures the philosophy of the empirical mode decomposition (EMD) (Huang et al, 1998) and sharpens the TF spectrum by squeezing the coefficients along the frequency axis. A generalized synchrosqueezing transform (GSST) (Li and Liang, 2012) and synchrosqueezing short-time Fourier transform (FSST) (Oberlin et al., 2014) have been put forward, respectively. Huang et al. (2016) proposed the synchrosqueezing S-transform (SSST) for seismic spectral decomposition and Wang et al. (2018) proposed the synchrosqueezing generalized S-

transform (SSGST), which inherits the advantages of SST and generalized S transform (GST). Compared with the SST based on STFT and CWT, the SSGST better reflects the TF characteristics of weak-amplitude and high-frequency data which is significant for hydrocarbon reservoir detection. It has been proved that the SST-based methods can provide an ideal TFR when addressing weak frequency modulation signal. However, most real signal, such as gravitational waves, speech, or seismic signal, are made up of strong frequency-modulated modes. To address this, the multi-synchrosqueezing transform (MSST) (Yu et al. 2019) was developed to extract more prominent features of a non-stationary signal. The MSST can be considered as an iterative SST procedure that reassigns the time-frequency coefficients to improve the energy concentration. The original MSST is based on the STFT, and the time-frequency resolution in seismic data analysis is fixed once the window length is preselected. Also low-amplitude and high-frequency features of seismic signals are not visible in MSST results.

Inspired by the MSST and GST procedure, we developed a new TF analysis method that was termed as MSST-GST. The MSST-GST is an extension of GST equipped with a multi-synchrosqueezing technique. In the GST, we employ a frequency-dependent Gaussian window with three parameters. The parameters can be adjusted adaptively to match the seismic signal in certain kinds of situations, which could provide an adaptive TF result and facilitate further interpretation. In the following section, we introduce the theory of MSST-GST in detail, then numerical examples are employed to illustrate the superior performance of MSST-GST over the ST-based and GST-based SST methods. Finally, field data applications further demonstrate the effectiveness of MSST-GST in highlighting geologic and stratigraphic information.

SYNCHROSQUEEZING GENERALIZED S TRANSFORM

$$ST_x(t,f)=\int_{-\infty}^{+\infty} x(\tau)h(\tau-t,f)\,\mathrm{e}^{-i2\pi f\tau}\,d\tau \quad , \tag{1}$$

where t and f are time and frequency, respectively, τ denotes the time shift and $h(t,f)$ is a frequency-dependent Gaussian window

$$h(t,f)=\frac{|f|}{\sqrt{2\pi}}e^{-\frac{t^2f^2}{2}} . \tag{2}$$

The inverse transform of ST is obtained by

$$x(t)==\int_{-\infty}^{+\infty}\int_{-\infty}^{+\infty} ST_x(\tau,f)\,\mathrm{e}^{i2\pi f\tau}\,d\tau df . \tag{3}$$

The ST can perform a multiresolution analysis as the window changes with increasing frequency, but the fixed window shape leads to a poor time resolution at low frequencies. In order to achieve a flexible TFR to characterize seismic features, the Gaussian window $h(t,f)$ can be generalized as

$$h(t,f,\mathrm{P}) = \frac{\sigma(f,P)}{\sqrt{2\pi}} e^{-\frac{t^2\sigma(f,P)^2}{2}} \quad , \tag{4}$$

where P represents the set of parameters and $\sigma(f,P)$ is the standard deviation of the generalized Gaussian window. In this work, the $\sigma(f,P)$ is defined as

$$\sigma(f,\{k,s,m\}) = k\left|f\right|^s + m \tag{5}$$

where $k>0, s>0,$ and $m>0$, k is the width factor which adjusts the width of the Gaussian window, m controls the tradeoff between the STFT and the ST, and s defines the change rate of window width with respect to frequency. The parameter set P are adaptively tuned to adjust the energy concentration of the TF result. The Renyi entropy (RE) was introduced to measure the energy concentration of the TFR, and the RE with α order is defined as

$$RE = \frac{1}{1-\alpha}\log_2 \frac{\iint_I \left|TFR(t,f)\right|^{2\alpha} dtdf}{(\iint_I \left|TFR(t,f)\right|^2 dtdf)^{\alpha}} \tag{6}$$

where I:=$(0,+\infty)\times(0,+\infty)$. It is well known that: the smaller the RE is, the more energy-concentrated the TFR is. In real application, the optimal parameters set P^* can be obtained by solving

$$P^* = \arg\min_P RE \quad , \tag{7}$$

using a cooperative coevolutionary differential evolution algorithm (Wang et al. 2018). Therefore, the GST can be expressed as

$$GST_x(t,f) = \int_{-\infty}^{+\infty} x(\tau)h(\tau-t,f,P)\,\mathrm{e}^{-i2\pi f\tau}\,d\tau. \tag{8}$$

According to the Parseval theorem, the GST can be rewritten in frequency domain as

$$GST_x(t,f) = \int_{-\infty}^{+\infty} X(\alpha+f)\,\mathrm{e}^{\frac{-2\pi^2\alpha^2}{\sigma^2(f,\mathrm{P})}}\mathrm{e}^{i2\pi\alpha t}\,d\alpha \tag{9}$$

where X is the Fourier transform (FT) of signal $x(t)$ and α is additional frequency variable. In order to calculate the instantaneous frequency function in SST, we consider a harmonic signal $h(t)=\mathrm{A}e^{i2\pi f_0 t}$, the FT of $h(t)$ is given as

$$\mathrm{H}(\alpha) = \mathrm{A}\,\delta(\alpha - f_0) \tag{10}$$

where δ denotes the Dirac delta function. Then the GST of harmonic signal $h(t)$ can be obtained by substituting eq. (10) into eq. (9)

$$GST_x(t,f) = A\,\mathrm{e}^{\frac{-2\pi^2(f-f_0)^2}{\sigma^2(f,\mathrm{P})}}\,\mathrm{e}^{i2\pi(f-f_0)t} \tag{11}$$

According to eq. (11), the instantaneous frequency of the harmonic signal $h(t)$ can be computed by taking first order derivative of GST with respect to variable t

$$\omega_x(t,f) = f + \frac{\partial_t GST(t,f)}{i2\pi\partial_t GST(t,f)} \quad . \tag{12}$$

Therefore, according the theories of SST, the synchrosqueezing generalized S-transform (SSGST) can be defined as

$$T_x(t,\hat{f}) = \int_{-\infty}^{+\infty} GST(t,f)\delta(\omega_x(t,f) - \hat{f})df \; . \tag{13}$$

Eq. (13) denotes that the time-frequency coefficients with the same instantaneous frequency $\omega_x(t,f)$ are superimposed on the frequency $\hat{f}$, so that we can obtain a sharp time-frequency representation.

MULTI-SYNCHROSQUEEZIN GENERALIZED S-TRANSFORM

In order to generate an energy-concentrated TF representation, the SST-based method assumes that the analyzed signal should be slowly time-varying. In real application, most signals are made up of strong frequency-modulated modes, as for instance, signals involved in speech processing, radar, or gravitational waves. The SST-based methods can not provide an accurate estimation of the instantaneous frequency in the analysis of signal that has strong frequency-modulated modes. To address this issue, the MSST was introduced to narrow the error between the true instantaneous frequency and the calculated instantaneous frequency by executing the synchrosqueezing operator multiple times, which lead to a more concentrated TF representation. The original MSST was proposed in the framework of STFT, and inspired by this, we integrated the generalized S-

transform (GST) into the MSST as a new method. We rewrite the formulation of SSGST as follows:

$$T_x^{[1]}(t,\hat{f}) = \int_{-\infty}^{+\infty} GST(t,f)\delta(\omega_x(t,f) - \hat{f})df \tag{14}$$

where the superscript of $T_x(t,\hat{f})$ represents the time of synchrosqueezing operator. After executing the synchrosqueezing operator twice, the second-order MSST-GST can be expressed as

$$\begin{aligned} T_x^{[2]}(t,\hat{f}) &= \int_{-\infty}^{+\infty} T_x^{[1]}(t,\eta)\delta(\omega_x(t,\eta) - \hat{f})d\eta \\ &= \int_{-\infty}^{+\infty}\int_{-\infty}^{+\infty} GST(t,f)\delta(\omega_x(t,f) - \eta)df \bullet \delta(\omega_x(t,\eta) - \hat{f})d\eta \\ &= \int_{-\infty}^{+\infty} GST(t,f)\int_{-\infty}^{+\infty} \delta(\omega_x(t,f) - \eta) \bullet \delta(\omega_x(t,\eta) - \hat{f})d\eta df \\ &= \int_{-\infty}^{+\infty} GST(t,f)\delta(\omega_x(t,\omega_x(t,f)) - \hat{f})df \end{aligned} \tag{15}$$

In eq. (15), the second-order MSST-GST makes use of a new instantaneous frequency function $\omega_x(t,\omega_x(t,f))$ to reassign the TF coefficients of GST. The $\omega_x(t,\omega_x(t,f))$ is closer to the true instantaneous frequency of signal than is the $\omega_x(t,f)$, which causes the second-order MSST-GST to produce a more concentrated result. Following this logic, the Nth-order of MSST-GST can be defined as

$$\begin{aligned} T_x^{[N]}(t,\hat{f}) &= \int_{-\infty}^{+\infty} T_x^{[N-1]}(t,\eta)\delta(\omega_x(t,\eta) - \hat{f})d\eta \\ &= \int_{-\infty}^{+\infty} GST(t,f)\delta(\omega_x^{[N]}(t,f) - \hat{f})df \\ &= \int_{-\infty}^{+\infty} GST(t,f)\delta(\omega_x(t,\omega_x(t,\omega_x(t,\mathrm{L}\ ,\ \omega_x(t,f)))) - \hat{f})df \end{aligned} \tag{16}$$

We can see that, the MSST-GST constructs a new instantaneous frequency estimate that reassigns the smeared result, and the instantaneous frequency estimate becomes closer and closer to the true instantaneous frequency. Therefore, the energy of the TF result will be concentrated in a stepwise manner.

The optimal TF resolution is not always required in seismic exploration. For instance, a better time localization is necessary in thin-bed detection and a better frequency resolution is required when estimating the tuning thickness of fluvial channels. Therefore, the proposed MSST-GST is suitable for different geologic goals.

NUMERICAL EXAMPLES

In this section, we compare the performance of MSST-GST and other existing methods. First, a test signal is employed to investigate the effectiveness of the proposed method

$$x(t) = \sin(2\pi(280t - 2e^{-3(\mathrm{t}-0.2)}\sin(15\pi(\mathrm{t}-0.2)) + \mathrm{sint})) \quad . \tag{17}$$

The time sampling interval is 2 ms. The TFRs generated by the GST and the MSST-GST are shown in Fig. 1(a-h), and the local zooms are displayed in the right side. In this experiment, the optimized parameter set P selected in the GST and MSST-GST is $P^*:\{k=0.6, s=0.8, m=9.2\}$. We can see the GST result, the TF spectrum illustrates a smearing result due to the uncertainty principle. In the SSGST result, the energy concentration is obviously improved. However, the energy leakage still exists because it cannot provide an accurate IF estimation when the signal has a strong FM behavior. For comparison, the TF features generated by second-order MSST-GST and fourth-order MSST-GST are clearer than that of ST and SSGST. Besides, the TF spectrum gets more and more concentrated as the increase of iterations.

A 3D field data is then used to investigate the application of the MSST-GST in seismic exploration. This is a 3D seismic data from the Bohai Basin in China, also analyzed by Wang and Gao (2014) and Liu et al. (2017). It contains 800 in-lines and 600 cross-lines. Each trace has 700 samples with a sampling interval of 2 ms. In this exploration area, the reservoir is mainly controlled by shallow-water deltaic systems and fluvial channels. Visualizing constant-frequency horizon slices of 3D data is a powerful tool to identify geologic structure that could be hidden in the original horizon amplitude map. Fig. 2(a) shows a time slice at 1220 ms of the 3D seismic cube which contains many fluvial channels, from the point of view of interpreter, knowing the extension and boundary of channels is important for reservoir characterization (Sinha et al., 2005). We apply the ST, SSGST, and fourth-order MSST-GST to all traces and compute the frequency where the cumulative spectral energy is 80 percent of the total energy. Time slices at 1220 ms are extracted after calculating constant frequency cubes.

Figs. 2(b)-2(d) show the resulting time slices for ST, SSGST, and fourth-order MSST-GST at 35 Hz, respectively. The channels are more sharply represented by SSGST and fourth-order MSST-GST than in the ST maps. SSGST and fourth-order MSST-GST have similar performances, however, the amplitude variations are better resolved in the fourth order MSST-GST due to the significantly reduced frequency smearing than for the SSGST methods (indicated by green rectangle).

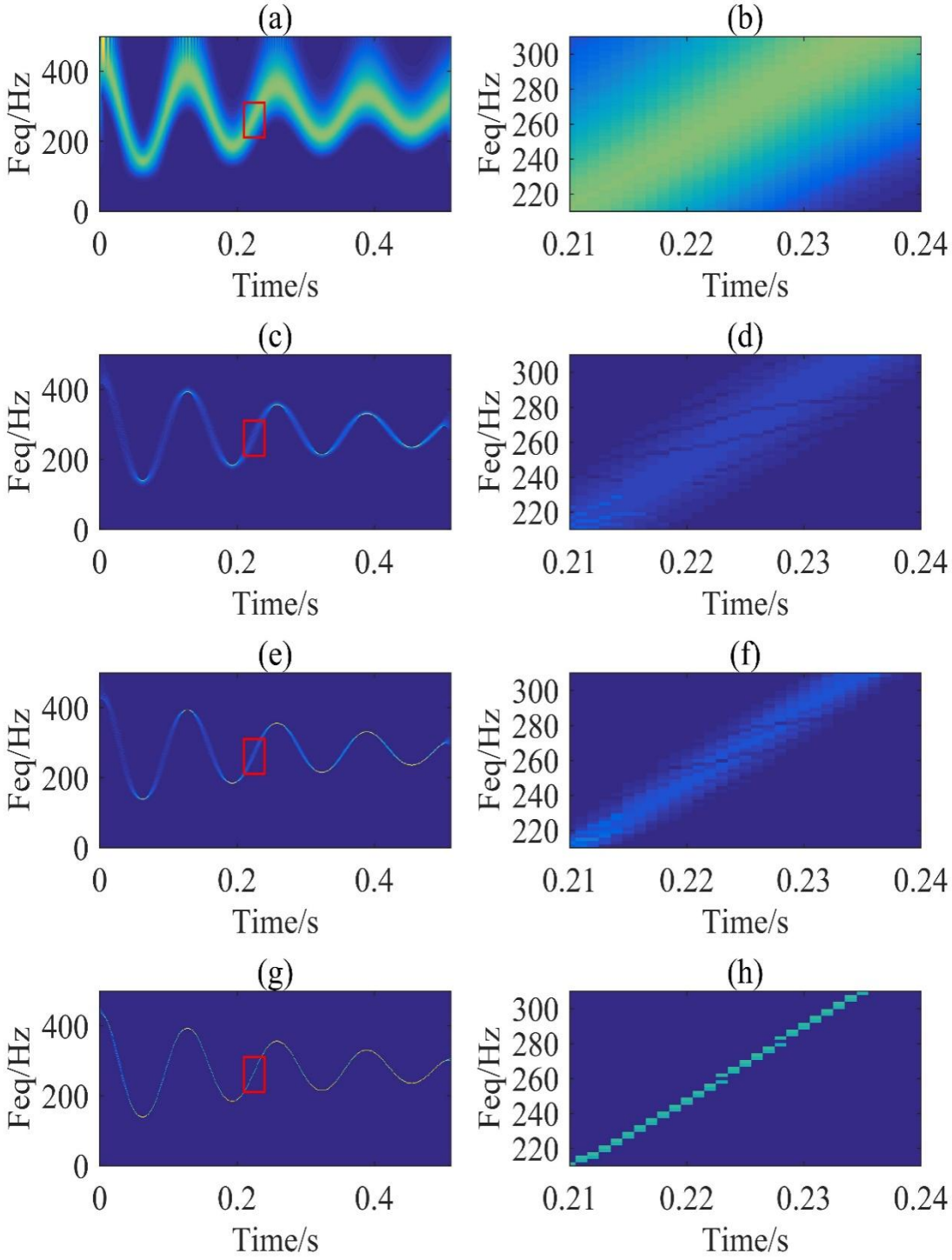

Fig. 1. Synthetic example. Time-frequency representations produced by (a) ST result, (b) the local zoom on ST result, (c) SSST result, (d) local zoom on SSST result, (e) second-order MSST-GST result, (f) local zoom on second-order MSST-GST result, (g) fourth-order MSST-GST result, (h) local zoom on fourth-order MSST-GST result.

To further demonstrate the performance of the MSST-GST method, we compare the decomposed frequency components on a 2D section with Inline number 1290 which is indicated by red line in Fig. 2. Fig. 3(a) shows the seismic section, we apply the three methods mentioned above to all traces and calculate the frequency where the cumulative spectral energy is at 80 percent of the total energy. We select the 2350th trace to optimize the parameters and the result is $P:\{k=0.78, s=1.05, m=3.7\}$. The 35-Hz constant frequency slices computed by ST, SSGST and fourth order MSST-GST are displayed in Figs. 3(b)-3(d). The black arrows with labels C1, C2 and C3 indicate three distinct channels which are indicated by yellow arrows in Fig. 2. In Fig. 3, the black curves are the gamma curves which demonstrate that the depositional settings of the primary reservoirs are dominated by the stacked fluvial channels and delta systems in several depositional cycles. In Fig. 3(b), the channel feathers are smeared which make the further interpretation difficult. In Fig. 3(c), due to its improved TF resolution, we can find that the SSGST highlights the channels. Compare with ST and SSGST, the result of fourth order MSST-GST characterizes the edges and the extension of the channels more clearly, which demonstrate that the MSST-GST can depict the geological structure with higher precision.

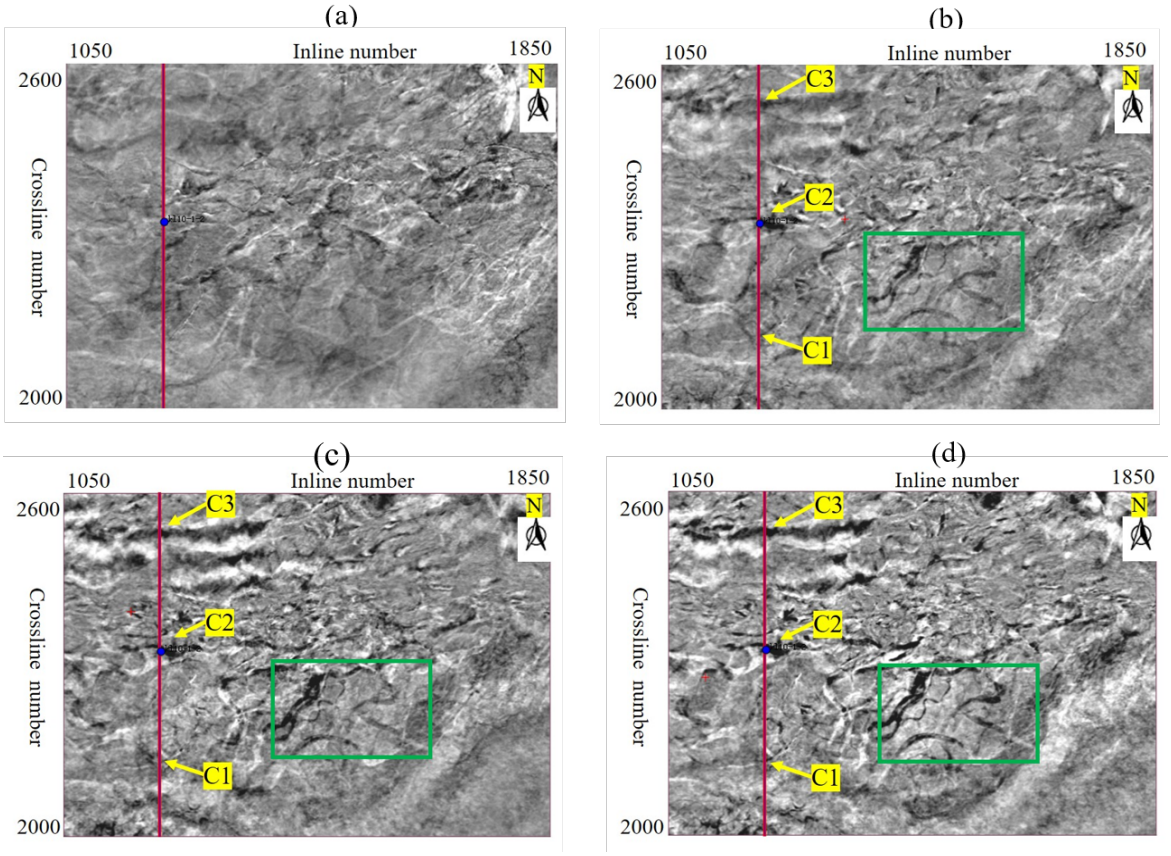

Fig. 2. Channel detection from horizontal slices. (a) Amplitude slice of the 3D original data. 35-Hz time slices computed using the (b) ST, (c) SSGST, (d) fourth order MSST-GST, respectively. Result based on fourth-order MSST-GST reveals more distinct channel features (indicated by the green rectangle), thus facilitating further interpretation.

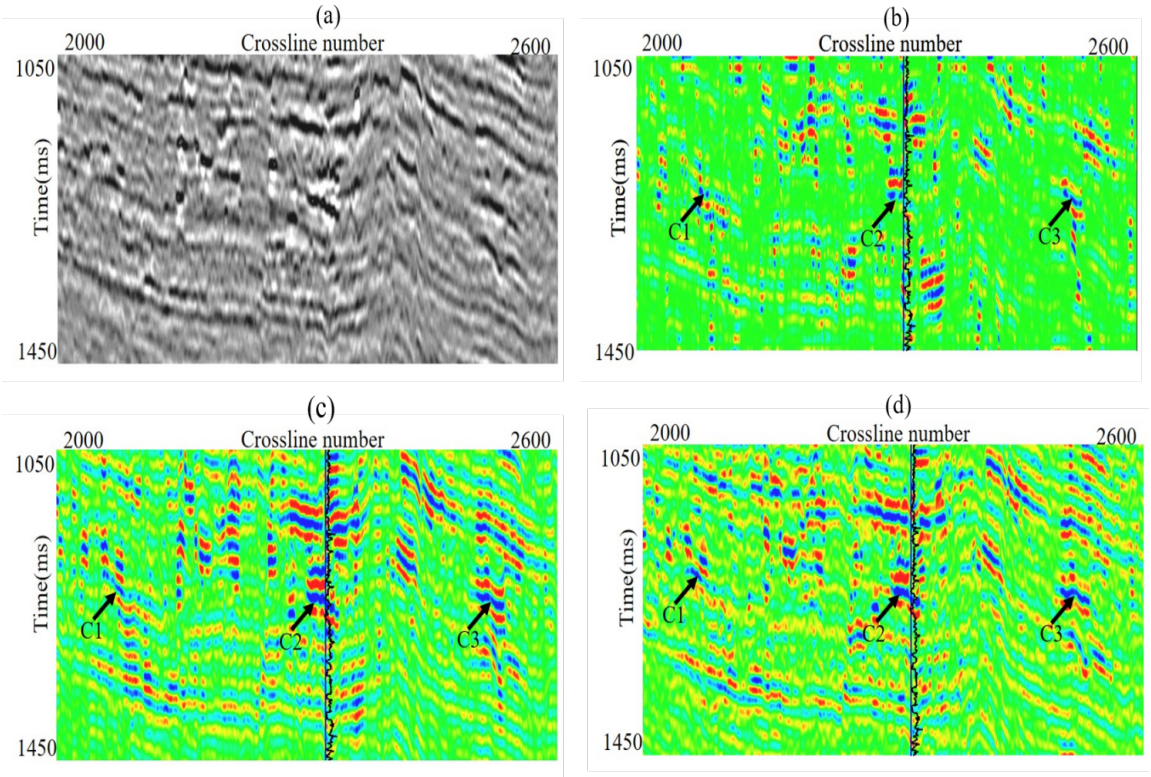

Fig. 3. Constant frequency spectral decomposition results of Inline1290. (a) The 2D seismic data at Inline 1290. 35-Hz spectral decomposition results calculated using the (b) ST (c) SSGST, and (d) fourth-order MSST-GST.

CONCLUSION

A more energy-concentrated time-frequency representation is significant for characterizing time-varying features of a seismic signal. In this paper, a new multi-synchrosqueezing algorithm, based on generalized S-transform, namely the MSST-GST method, is proposed for seismic time-frequency analysis. In the MSST-GST method, an iterative reassignment procedure is used to improve the instantaneous frequency estimation and the energy concentration of the time-frequency representation. The advantages of the MSST-GST are demonstrated through numerical examples and the effectiveness of the MSST-GST for geological structure depiction is confirmed by real data applications.

ACKNOWLEDGEMENTS

This work was financially supported by the excellent young and middle-aged science and Technology Innovation team project of the Education Department of Hubei Province (No. T2022029).

REFERENCES

Auger, F. and Flandrin, P., 1995. Improving the readability of time-frequency and time-scale representations by the reassignment method. IEEE Trans. Signal Process., 43: 1068-1089.

Chakraborty, A. and Okaya, D., 1995. Frequency-time decomposition on seismic data using wavelet-based methods. Geophysics, 60: 1906-1916.

Daubechies, I., Lu, J. and Wu, H., 2011. Synchrosqueezed wavelet transform: An empirical mode decomposition-like tool. Appl. Comput. Harmon. Anal., 30: 243-261.

Ebrom, D., 2004. The low-frequency gas shadow on seismic section. The Leading Edge, 23: 772.

Huang, N.E., Shen, Z., Long, S.R., Wu, M.C., Shih, H.H., Zheng, Q., Yen, N-C., Tung, C.C. and Liu, H.H., 1998. The empirical mode decomposition and the Hilbert spectrum for nonlinear and nonstationary time series analysis. Proc. R. Soc. Lond. A, 454: 903-995.

Huang, Z., Zhang, J., Zhao, T. and Sun, Y., 2016. Synchrosqueezing S-transform and its application in seismic spectral decomposition. IEEE Transact. Geosci, Remote Sensing., 54: 817-825.

Jeffrey, C. and William, J., 1999. On the existence of discrete Wigner distributions. IEEE Signal Process. Lett., 6: 304-306.

Li, C. and Liang M., 2012. A generalized synchrosqueezing transform for enhancing signal time-frequency representation. Signal Process., 92: 2264-2274.

Liu, N., Gao, J., Zhang, Z., Jiang, X. and Lv, Q., 2017. High-resolution characterization of geologic structures using the synchrosqueezing transform, Interpretation, 5: T75-T85.

Oberlin, T., Meignen, S. and Perrier, V., 2014. The Fourier-based synchrosqueezing transform. ICASSP, Italy: 315-319.

Reine, C., van der Baan, M. and Clark, R., 2009. The robustness of seismic attenuation measurements using fixed- and variable-window time-frequency transform. Geophysics, 74: 123-135.

Sinha, S., Routh, P.S., Anno, P.D. and Castagna, J.P., 2005. Spectral decomposition of seismic data with continuous wavelet transform. Geophysics, 70: 19-25.

Stockwell, R., Mansinha, L. and Lowe, R., 1996. Localization of complex spectrum: The S-transform. IEEE Transact. Signal Process., 44: 998-1001.

Wang, Q., Gao, J., Liu, N. and Jiang, X., 2018. High-resolution Seismic Analysis Using the Synchrosqueezing Generalized S-Transform. IEEE Geosci. Remote Sens. Lett., 15: 374-378.

Wang, C., Gao, J., 2018. High-dimension waveform inversion with cooperative coevolutionary differential evolution algorithm. IEEE Geosci. Remote Sens. Lett., 19: 297-301.

Wang, P., Gao, J. and Wang, Z., 2014. Time-frequency analysis of seismic data using synchrosqueezing transform. IEEE Geosci. Remote Sens. Lett., 11: 2042-2044.

Yu, G., Wang, Z. and Zhao, P., 2019. Multisynchrosqueezing transform. IEEE Transact. Ind. Electron, 66: 5441-5455.